J Neuroimmune Pharmacol (2015) 10:88–101
DOI 10.1007/s11481-014-9576-7

ORIGINAL ARTICLE

Amphiphilic Cationic Nanogels as Brain-Targeted Carriers for Activated Nucleoside Reverse Transcriptase Inhibitors

G. Warren · E. Makarov · Y. Lu · T. Senanayake · K. Rivera · S. Gorantla · L. Y. Poluektova · S. V. Vinogradov

Received: 15 September 2014 / Accepted: 18 December 2014 / Published online: 6 January 2015

Abstract Progress in AIDS treatment shifted emphasis towards limiting adverse effects of antiviral drugs while improving the treatment of hard-to-reach viral reservoirs. Many therapeutic nucleoside reverse transcriptase inhibitors (NRTI) have a limited access to the central nervous system (CNS). Increased NRTI levels induced various complications during the therapy, including neurotoxicity, due to the NRTI toxicity to mitochondria. Here, we describe an innovative design of biodegradable cationic cholesterol-ε-polylysine nanogel carriers for delivery of triphosphorylated NRTIs that demonstrated high anti-HIV activity along with low neurotoxicity, warranting minimal side effects following systemic administration. Efficient CNS targeting was achieved by nanogel modification with brain-specific peptide vectors. Novel dual and triple-drug nanoformulations, analogous to therapeutic NRTI cocktails, displayed equal or higher antiviral activity in HIV-infected macrophages compared to free drugs. Our results suggest potential alternative approach to HIV-1 treatment focused on the effective nanodrug delivery to viral reservoirs in the CNS and reduced neurotoxicity.

Keywords HIV-1 · Nucleoside reverse transcriptase inhibitors · Nanogels · ε-polylysine · NRTI 5′-triphosphates · Zidovudine · Lamivudine · Abacavir · Central nervous system · Brain-specific peptides · Blood–brain barrier · Neurotoxicity

G. Warren · Y. Lu · T. Senanayake · K. Rivera · S. V. Vinogradov (✉)
Department of Pharmaceutical Sciences, University of Nebraska Medical Center, Omaha, NE, USA
e-mail: vinograd@unmc.edu

E. Makarov · S. Gorantla · L. Y. Poluektova
Department of Pharmacology and Experimental Neuroscience, University of Nebraska Medical Center, Omaha, NE, USA

Abbreviations

ApoE	Apolipoprotein E
B	Abacavir
BP	Brain-specific peptide
BBB	Blood–brain barrier
CEPL	Cholesteryl-EPL
CNS	Central nervous system
EPL	Epsilon-polylysine
GLN	Glutathione
HIV	Human immunodeficiency virus
L	Lamivudine
MDM	Monocyte-derived macrophages
NRTI	Nucleoside reverse transcriptase inhibitors
NG	Nanogel (PEG-CEPL)
PEG	Poly(ethylene glycol)
RT	Reverse transcriptase
Z	Zidovudine (AZT)

Introduction

Modern antiretroviral therapy includes multi-drug treatment with NRTIs as an integral part of many antiviral cocktails. Despite the reduction of viral load and improvement of HIV infected patients' quality of live, chronic antiviral treatment was often associated with adverse effects, including neurotoxicity. Significant limitation of many antiviral drugs is their inefficient CNS accumulation due to the poor blood–brain barrier (BBB) permeability (Pialoux et al. 1997). Development of HIV-associated encephalitis and neurodegeneration in the CNS accelerates neuronal death and degradation of cognitive skills (Lindl et al. 2010). The principal cause of neurotoxicity is NRTI-related mitochondrial toxicity (Lewis et al. 2003). Once in the CNS, NRTI drugs penetrate neurons and inhibit replication of mitochondrial DNA (mtDNA). This deficit affects ATP production and results in insufficient

energy to maintain cellular homeostasis, which leads to neuronal death. Limiting the NRTI access to mitochondria can potentially reduce these side effects. Permeability of mitochondrial membrane depends on the charge and hydrophobicity of drugs, therefore, hydrophilic and negatively charged compounds have low permeability.

NRTI are inactive prodrugs that have to be converted into active 5′-triphosphates (NTP) by cellular kinases. Activated drugs can inhibit HIV-1 reverse transcriptase (RT) activity by incorporating into viral genome. Accumulation of NRTI inside the infected cells also inhibits DNA polymerase γ involved in the synthesis of mtDNA (Lewis et al. 2003). Cellular delivery of NTP would increase the efficiency of anti-viral drugs by skipping the phosphorylation of its prodrugs. Unfortunately, 5′-triphosphates are unstable in serum and require nanoencapsulation for successful in vivo delivery. Cationic nanogels were found to be an effective drug delivery system for nucleoside 5′-triphosphates (Vinogradov et al. 2005a). Cationic nanogels neutralize negative charge of NTP and enhance cellular penetration via adsorptive endocytosis. After the fusion of loaded nanogel (NG/NTP) with cellular membrane, 5′-triphosphorylated drug are readily released into the cytosol (Vinogradov et al. 2005b). Once inside the cells, penetration of NTP molecules into mitochondria was limited due to negative charge of these drugs, thus preserving mitochondrial function. In addition, loaded nanogels had lesser effect on the polarization of mitochondrial membrane compared to free NRTI (Kohli et al. 2007). Thus, NG/NTP nanodrugs can provide additional benefits in reducing mitochondrial toxicity of NRTI drugs.

In order to ensure sufficient brain accumulation of therapeutic NRTIs, administration of elevated drug doses was required resulting in unsolved toxicity concerns. In recent years, various approaches to deliver drugs into the CNS using different receptors on the BBB endothelium demonstrated their practical potential (Tiwari and Amiji 2006; Zensi et al. 2009). Peptide molecules showed a special promise for targeted brain delivery via systemic drug administration (Delehanty et al. 2010; Li et al. 2011; Gerson et al. 2014). In the CNS, HIV-1 resides mostly in microglia or macrophages, however, other brain-associated cells may become infected with HIV-1 in vivo with variable levels of HIV-1 mRNA expression. The diverse cellular reservoirs for HIV-1 in the CNS may be critically linked to the molecular mechanisms involved in HIV-1 neuropathogenesis, for example, in vivo infection of the BBB endothelial cells, and possibly cells in the choroid plexus, may directly contribute to penetration of the BBB by HIV-1 (Bagasra et al. 1996). Recently, we demonstrated the strong potential of LDL receptor-specific ApoE peptide-modified NG/NTP for the treatment of HIV-1 infection in the CNS using a humanized HIV mouse model (Gerson et al. 2014). In this approach, 10-fold reduction in RT activity in the brain was achieved by accumulation of therapeutic levels of nanogel-formulated Zidovudine 5′-triphosphate (ZTP) after systemic administration.

In the current study, we designed and evaluated novel type of nanocarriers based on the biodegradable epsilon-polylysine (EPL), an FDA approved natural food preservative that belongs to the group of cationic biopolymers. We prepared and investigated antiviral efficacy of BBB-targeted peptide-NG/NTP formulations of Zidovudine (Z), Lamivudine (L) and Abacavir (B), as well as dual (Z+L) and triple (Z+L+B) nanodrug cocktails in HIV-1 infected macrophages. After comparison with corresponding NRTI and NRTI cocktails, NG/NTP demonstrated lower neurotoxicity and mitochondrial toxicity than free drugs and efficiently accumulated in monocyte-derived macrophages (MDM), suppressing HIV-1 RT activity in these cells. Attachment of brain-targeting peptides allowed us to substantially increase the CNS accumulation of NG/NTP formulations without compromising their antiviral activity. The outline of nano-NRTI approach to eradication of HIV infection in the CNS is shown in Fig. 1. Briefly, nanodrugs infused in blood circulation selectively bind to the brain vascular endothelium and efficiently penetrate the BBB via transcytosis due to their very small size. On basolateral side, brain phagocytes (macrophages, astrocytes and microglia) are able to collect nanodrug particles, which successfully release the activated NRTI molecules inside the cells. The intracellular therapeutic level of NRTI drugs is maintained for several days and results in the active inhibition of HIV-1 proliferation in the infected immune cells.

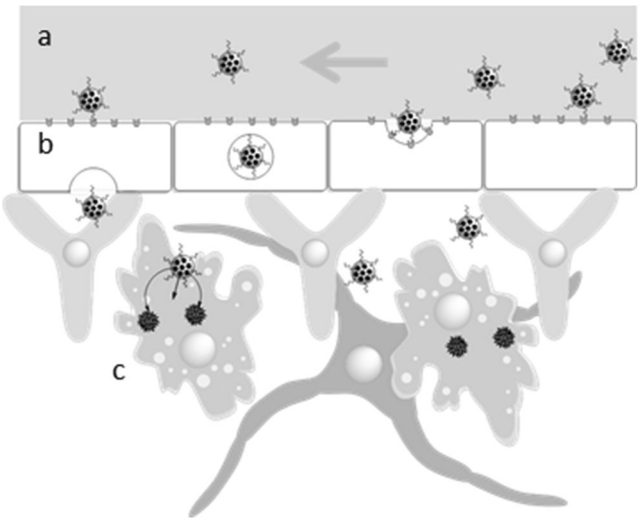

Fig. 1 Outline of the nano-NRTI strategy against HIV infection in the CNS. **a** Targeted delivery of nanodrugs (NG/NTP) from the blood to the brain endothelium, **b** penetration through the BBB by transcytosis, **c** phagocytic capture of nanodrugs and release of active NRTI drugs for suppression of HIV-1 infection

Materials and Methods

Chemicals

All reagents, if not mentioned separately, were purchased from Sigma-Aldrich (St Louis, MO) and used without additional purification. Maleimide-PEG_{3500}-NHS and $mPEG_{3500}$-NHS esters were obtained from GenKem Technology USA (Allen, TX). Abacavir, Lamivudine, and 3′-azido-3′-deoxythymidine (Zidovudine) have been purchased from Carbosynth Inc (Compton, Berkshire, UK). N-Succinimidyl [2,3-^{3}H] propionate was obtained from Moravek Radiochemicals (Brea, CA). NAP columns for gel filtration were purchased from GE Healthcare Biosciences (Piscataway, NJ). Dialysis tubes were obtained from Thermo Fisher Scientific (Waltham, MA). Peptides having a N-cysteine residue and protected C-amino acid amide have been custom synthesized by Biomer Technology (Pleasanton, CA) and used directly after short dialysis (MWCO 500) against degassed water, or after purification by reverse-phase HPLC depending on synthetic purity. The sequences of synthetic peptides are as follows: CGLRKMRKRLMR (ApoE) (Sauer et al. 2005); CGNAFTPDY (BP1) and CGKAAQVYG (BP2) (Sadanandam et al. 2007); and CGTGNYKALHPHNG (TGN) (Li et al. 2011).

Cell Lines

Human HepG2 hepatocellular carcinoma cells were purchased from American Type Culture Collection (Manassas, VA) and cultivated in Eagle's Minimal Essential Medium (MEM, Corning Cellgro) containing 10 % heat-inactivated fetal bovine serum (FBS) supplemented with streptomycin (5 μg/ml). Human A172 astroglial cells (ATCC) have been utilized in various pharmacology- and neurochemistry-based studies as a common model of astrocytes. A172 cells were cultivated in Dulbecco Modified Eagle Medium (DMEM, Life Technologies) with high glucose, supplemented with glutamine (4 mM) and 1 % penicillin-streptomycin, and containing 10 % FBS. Human SH-SY5Y neuroblastoma cells (ATCC) are widely used as a neuronal model and possess many biochemical and functional properties of neurons. SH-SY5Y cells were cultured in a 1:1 mixture of MEM and F12 medium containing nonessential amino acids (Gibco), 1 % penicillin-streptomycin, and supplemented with 10 % FBS. Murine brain capillary endothelial cell line bEnd.3 (ATCC) was cultivated in DMEM supplemented with 2 % penicillin-streptomycin and 10 % FBS. Cell passages from 32 to 35 were used for transport experiments. Murine BV-2 microglial cells (Common Access to Biological Resources and Information, cabri.org) retain the phenotypic and functional characteristics of primary microglial cells (Henn et al. 2009). BV-2 cells were cultivated in DMEM with high glucose, containing 10 % FBS and supplemented with glutamine (4 mM) and 1 % penicillin-streptomycin. All cells were cultured in water-saturated 5 % CO_2 atmosphere at 37 °C. Cells from primary rat neuron kit (Brain Bits, Springfield, IL) were seeded in poly-D-lysine covered plates and cultured for 3 days in the company-supplemented NbActiv1 growth medium before treatment.

Primary human monocytes were obtained from leukopheresis of HIV-seronegative donors and differentiated into MDM as previously described (Vinogradov et al. 2010). Cells were cultured in DMEM supplemented with 10 % heat-inactivated pooled human serum and 1 % glutamine, 10 mg/mL ciprofloxacin and 1000 U/mL of purified recombinant human macrophage colony-stimulating factor (R&D Systems, Minneapolis, MN). A macrophage-tropic viral strain HIV-1_{ADA} at a multiplicity of infection (MOI) of 0.01 was amplified and used as previously described (Nukuna et al. 2004).

Synthesis of Nanogels

Epsilon-polylysine (EPL, M.w. 4600) was dissolved in anhydrous DMF and treated dropwise with an equal volume of cholesteryl chloroformate solution in anhydrous dichloromethane (reagent/EPL molar ratio 3). After overnight stirring at 25 °C, the mixture was concentrated *in vacuo*, and a slightly yellow viscous product was dissolved in water and titrated with 1 M hydrochloric acid to pH 7. The aqueous solution was centrifuged to remove any unbound cholesterol, dialyzed against water (2×3 h), and then sonicated for 1 h in ice bath to obtain compact nanogel particles before the next step of modification. The CEPL nanogels were treated with a 2-fold weight excess of $mPEG_{3500}$-NHS or MAL-PEG_{3500}-NHS added as an aqueous solution dropwise, and the modification was continued under argon for 1 h at 25 °C. Peptides dissolved in 50 % DMF under argon were added dropwise to the MAL-PEG_{3500}-CEPL nanogel solution adjusted to pH 6. Usually, a two-fold molar excess of the peptide (over MAL moieties) was used in the overnight reaction at 4 °C, and then any unreacted MAL moieties were capped with 10 mM cysteine solution for 1 h. Final products have been dialyzed twice for 24 h against water at 4 °C using membranes with MWCO 4000–8000 Da. Peptide content in nanogels was determined using amino acid analysis after acidic degradation (UNMC Protein Analysis Core). The hydrodynamic diameter (d_h) of nanogels was analyzed in 1 % solutions in PBS by dynamic light scattering (DLS) using Malvern ZetaSizer Nano-ZS90 (Table 1).

Synthesis of NRTI 5′-triphosphates (NTP)

NRTI have been efficiently converted into 5′-triphosphates using a 'one-pot' synthetic approach reported in details previously (Vinogradov et al. 2005a). Exocyclic amino group of Lamivudine was protected by isobutyryl moiety using a

Table 1 Properties of nanogels and NG/NTP formulations

Nanogel	d_h, nm[a]	d_h, nm (+ZTP)[a]	PDI[a]	ZTP, μmol/mg[b]
NG	18±1	12±2	0.30	0.34±0.04
ApoE-NG	35±9	31±2	0.40	0.22±0.01
BP2-NG	32±3	29±3	0.35	0.25±0.02
GLN-NG	29±2	27±1	0.33	0.27±0.01

[a] Hydrodynamic diameter, d_h, and polydispersity index, PDI, measured by light scattering

[b] ZTP content (per 1 mg of nanodrug) calculated from UV absorbance of NG/ZTP solutions

transient protection by trimethylsilyl moiety (Senanayake et al. 2013). Each nucleoside analog dissolved in dry dimethylformamide (DMF) was treated with a 1.5-molar excess of *tris*-triazolyl phosphate reagent for 30–60 min at 4 °C, and then added dropwise to the excess of tri-n-butylammonium pyrophosphate in dry DMF. After overnight reaction at 25 °C, an equal volume of cold 0.2 M triethylammonium bicarbonate was added. After 30 min, the mixture was dialyzed (MWCO 500) against water overnight at 4 °C. The desalted NTP solution was concentrated *in vacuo* and precipitated in 2 % sodium perchlorate in acetone in the form of sodium salt. Total NTP yields were 65–80 %. The drug content of purified NTP (ZTP, LTP and BTP) was no less than 90 % by UV absorbance at 260 nm (NRTI content), and 75 % on the base of ion-pair HPLC peak corresponding to 5′-triphosphate (NTP content). All products have been analyzed by UV and ^{1}H-NMR spectra.

Formulation of Nanodrugs (NG/NTP) and In Vitro Drug Release

To formulate nanodrugs, aqueous solution of cationic nanogels (NG) and ZTP, LTP or BTP were mixed at nanogel-to-triphosphate weight ratio 4. After incubation on ice for 30 min, unbound drug was removed by gel filtration on NAP-10 column. The NG/NTP products were lyophilized and stored at 4 °C before applications. Aqueous solutions of NG/NTP have been analyzed by UV absorbance to determine the drug content using the following extinction coefficients: ε_{260} 9200 (Abacavir), ε_{260} 9480 (Lamivudine), and ε_{260} 11, 250 (Zidovudine). The DLS particle size (d_h) and polydispersity index (PDI) of nanodrugs are shown in Table 1. To determine kinetics of an in vitro drug release, a NG/NTP formulation was incubated in Dia-Lo-tubes (MWCO 2000 Da) placed in the 1 L-beaker containing PBS with 0.05 % sodium azide at 25 °C (daily change of the medium). Samples taken from the tubes at different time intervals were analyzed by UV absorbance at 260 nm. The curves have been plotted as a percentage of drug release versus time.

Cytotoxicity

Cytotoxicity of NG/NTP formulations was evaluated using an MTT assay as previously described (Gerson et al. 2014). Initially, cells were treated for 4 h at 37 °C to allow the internalization of NG/NTP, then the treatment solution was washed out, and cells were incubated for additional 20 h at 37 °C. The MTT assay was also used in the measurements of viral RT activity in cultured MDM infected with HIV-1 in order to normalize data by functional levels of live cells.

Cellular Accumulation

Nanogels were tagged with Rhodamine (Rh) isothiocyanate and purified using a NAP-10 column as previously described (Gerson et al. 2014). Fluorescent nanogels loaded with NTP (Rh-NG/NTP) at concentrations of 10 and 50 μg/mL were used to treat MDM suspension (1×10^6 cells/mL) in full cellular medium. At appropriate time intervals, the cells were washed with cold PBS and treated with propidium iodide for 15 min at 4 °C and analyzed by fluorescence-activated cell sorting (FACS). The percentage of live cells and the mean fluorescent intensity was measured using FACS Array Bioanalyzer (BD Bioscience, Franklin Lakes, NJ). For cellular biodistribution studies, Rh-NG was loaded with a fluorescent triphosphate, ATP *BODIPY FL* (Molecular Probes, Invitrogen). MDM were treated separately with 25 μg/mL Rh-NG and Rh-NG/ATP *BODIPY FL* formulation in full cellular medium for 1 h at 37 °C, then washed several times with cold PBS and centrifuged. Confocal microscopy of the cells fixed with paraformaldehyde was performed in covered chamber slides using a Zeiss 410 Confocal Laser Scanning Microscope equipped with an argon-krypton laser.

Apoptosis in Neural Cells

Annexin V Apoptosis assay (Clontech Laboratories) was used to measure apoptosis in SH-SY5Y neural cells. The cells (2×10^5 per well) were pretreated with NG/NTP (200 μg/mL) or NRTI (20 μg/mL) in duplicates for 4 h at 37 °C. Then, the treatment solution was removed and a fresh full medium was added, and cells were incubated for other 24 h. Cells washed with PBS twice have been treated with trypsin solution to detach them and pelleted (1100 rpm, 5 min, 4 °C). To cells resuspended in 250 μL of Binding buffer a 2.5 μL of Annexin V-FITC was added and tubes were incubated for 10 min at 25 °C. Cells were washed with ice-cold PBS to remove non-bound Annexin V-FITC and pelleted (1100 rpm, 5 min, 4 °C). Resuspended in 500 μL ice-cold PBS cells have been analyzed immediately and the percentage of apoptotic cells was measured using FACS Array Bioanalyzer.

Mitochondrial Toxicity

Effect of the extended treatment of hepatic HepG2 cells with NRTI and NG/NTP on the amount of mtDNA was measured as previously described (Vinogradov et al. 2010). Cells were treated with sterile solutions of AZT and NG/ZTP formulations, 30 and 300 μg/mL, respectively, in full medium for 4 h at 37 °C on Days 1, 4, 7 and analyzed on Day 10. After trypsinolysis and treatment with RNase, DNA samples were isolated as previously described and analyzed by real-time PCR. Human cytochrome *b* gene primers (mtDNA): 5′-CCAACATCTCCGCATGATGAAAC-3′ (direct) and 5′-GTGGGCGATTGATGAAAAGG-3′ (reverse), and β-actin gene primers (nuDNA): 5′-AACACCCCAGCCATGTACGT-3′ (direct) and 5′-TCTCCTTAATGTCACGCACGA-3′ (reverse) were applied to quantify the amount of mtDNA and nuDNA (Höschele et al. 2008). Mini-iQ Real-Time PCR detection system (BioRad, Hercules, CA) and Evagreen Supermix at the conditions recommended by the manufacturer have been used in the analysis. The results were calculated as the mtDNA/nuDNA ratio=$2^{-C(t)mt}/2^{-C(t)nu}$, where $C(t)_{mt}$ and $C(t)_{nu}$ are the quantification cycles observed for mtDNA and nuDNA in each sample. The ratio in non-treated cells was taken for 100 %, and all obtained data were expressed as the percentage change compared to non-treated cells.

ROS Assay

Production of the reactive oxygen species (ROS) in MDM was measured using an OxiSelect ROS assay kit (Cell Biolabs). The cells were treated with NG/ZTP (4 μg/mL) in growth medium for 24 h. Hydrogen peroxide (H_2O_2 40 μM) was applied for 24 h as a positive control. Non-treated cells served as a negative control. All cells were washed twice with PBS, and a dichloro-dihydro-fluorescein diacetate dissolved in growth medium was added and incubated for 1 h at 37 °C. Washed with PBS cells were treated by adding 100 μL of Cell Lysis Buffer for 5 min at 20 °C, and the fluorescence was measured using a FLx-800 plate reader (BioTek USA, Vinooski, VT) and analyzed by KC Junior software.

Antiviral Activity

Human MDM were cultured for 7 days in 96-well plates, changing culture medium every other day. NG/NTP and NRTI were dissolved in sterile deionized water to obtain 20× stock solutions. In sterile 96-well plate, 10 μl of 20× stock solutions were mixed with 190 μl of complete culture medium, and serial 1/2 dilutions (100 μl) were prepared. On Day 7, old medium was removed and supplemented with the serial dilutions. Plates were incubated for 4 h at 37 °C and 5 % CO_2. After incubation, cells were washed with PBS, and the fresh media containing 0.01 MOI of HIV-1_{ADA} was added for the overnight (16 h) infection. Infected MDM were washed and supplemented with a fresh medium. On Day 5 and 7 post-infection, supernatants were collected for the RT activity assay. Each plate contained infected but non-treated and uninfected cell controls. All nanodrugs and controls were analyzed in 5 parallels.

To measure HIV-1 replication, reverse transcriptase (RT) activity was determined by incubating 10 μL of infected sample media with a reaction mixture consisting of 0.05 % Nonidet P-40 (Sigma-Aldrich) and [^{3}H]dTTP (2 Ci/mmol; Moravek, Brea, CA) in *Tris–HCl* buffer (pH 7.9) for 24 h at 37 °C on days 5 and 7 post-infection (Nukuna et al. 2004). Radiolabeled DNA was precipitated on paper filters in an automatic cell harvester (Skatron, Sterling, VA) and incorporated activity was measured by liquid scintillation spectroscopy. The cytotoxicity of NG/NTP and NRTI was determined on Day 7 using an MTT assay as previously described. The mean OD_{490} values for non-treated controls were taken for 1, and the cytotoxicity data have been converted to obtain the normalization factors. All observed HIV-1 RT activity values were normalized by these factors and plotted as a function of NG/NTP or NRTI concentrations. Antiviral efficacy was expressed as the effective drug concentration that inhibited HIV-1 RT activity by 90 % (EC_{90}) and was determined from concentration-effect curves generated using GraphPad Prism 4.03 (GraphPad Software, San Diego, CA).

Transport Across the BBB

Murine brain capillary endothelial cells bEnd3 have been grown until confluency on the semi-permeable membrane of Transwell inserts (24-well plate) treated with Matrigel according to the protocol (Simon et al. 2010). Trans-endothelial electrical resistance (TEER) was measured on Day 5 using E-VOM2 Epithelial Voltmeter (World Precision Instruments, Sarasota, FL). Confluent monolayers had resistance values ≥33 Ωcm^2. Upper Transwell compartment (apical side) medium containing 10 % FBS was mixed with stock nanogel solution. The lower Transwell compartment (basolateral side) contained fresh serum-free medium. Plates were incubated for 0.5, 1, 2 and 4 h at 37 °C, when fluorescence of basolateral solution was measured at *ex* 590 nm/*em* 620 nm in black-walled plate in duplicates. Results have been analyzed and P_{app} calculated using the following equation: $P_{app}=(dx/dt)/(0.33\times C_o\times 60\times 60)$(cm/s), where x is the nanogel accumulation on the basolateral side during 1 h-incubation, C_o is the initial nanogel concentration on the apical side, and 0.33 is the filter area in cm^2.

Brain Accumulation

Nanogel samples have been labelled with N-succinimidyl [^{3}H]-propionate (Moravek, Brea, CA) as previously described (Vinogradov et al. 2004a). Each ^{3}H-NG/CTP formulation was injected in the tail vein of C57BL/6 mice (3 animals per group), and its amount in blood and organs (brain, liver, spleen, kidney, lung and heart) was measured at different doses and time points. Organs were analyzed by dissolving in 1 mL Solvable solution (Perkin Elmer, Santa Clara, CA) per 100 mg tissue for 1 h at 60 °C. Samples were treated with 0.1 mL of 0.2 M EDTA and 0.2 mL of hydrogen peroxide (30 % v/v) overnight, and then mixed with 0.1 mL of 1 N HCl. Half of the tissue solution was added to 2 mL of Ultima Gold Scintillation Mixture (Perkin Elmer) in glass scintillation vial, and the sample radioactivity was measured using a 2500TR/RB Packard Tricarb liquid scintillation analyzer (Perkin Elmer).

Results

Vectorized Nanogel Carriers

Ultra small nanogel carriers (d~20 nm) could be prepared from self-assembling spherical cationic CEPL polymer network modified with short PEG molecules (Fig. 2a). The cationic nanogel network is easily accessible to small NTP molecules in aqueous solution and could be loaded by simple mixing both nanogel and NTP drug solutions Vinogradov et al. (2005b). For drug delivery to the brain, we synthesized novel cholesteryl-EPL (CEPL) nanogel carriers of very small size based on the biodegradable ε-polylysine polymer, which was recently approved for certain human applications (Hunter and Moghimi 2010). Optimal cholesterol content in order to ensure the efficient cellular uptake of PEGylated cationic nanogels was found to be in the range of 3–7 % or three

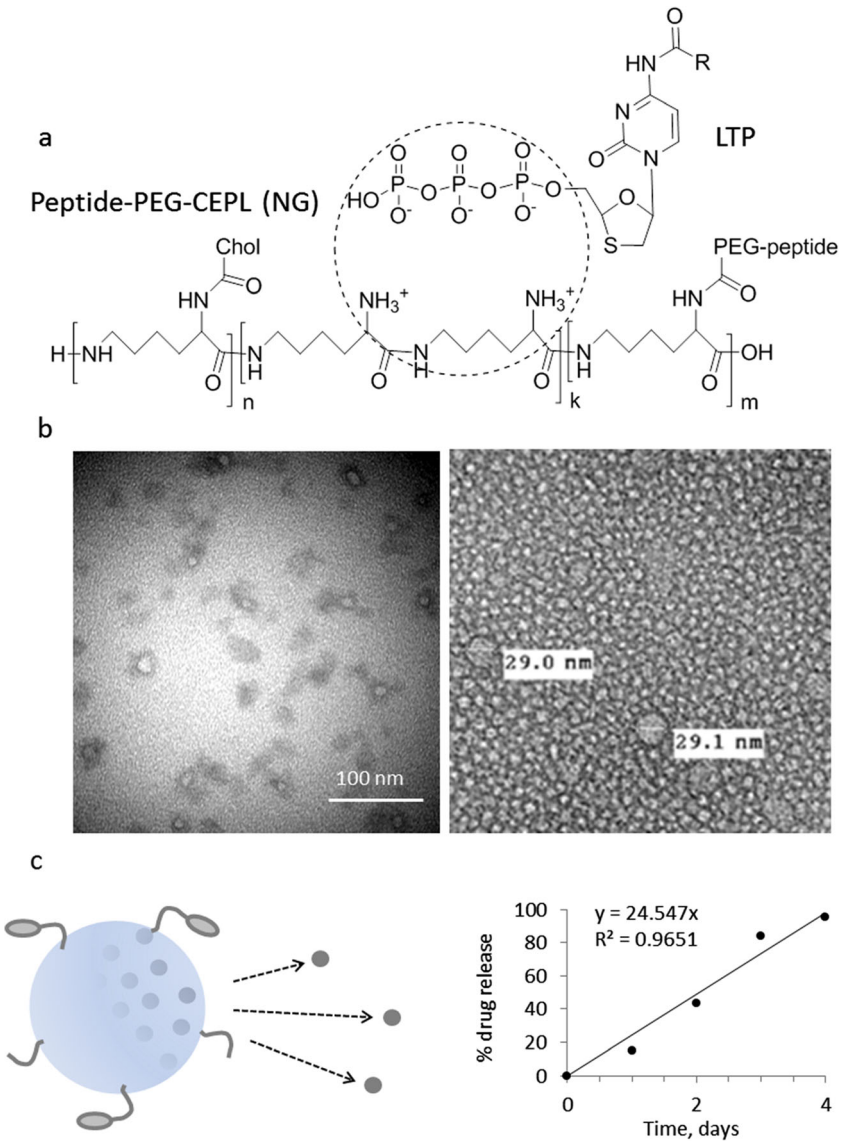

Fig. 2 **a** Chemical structures of peptide-PEG-CEPL nanogel (*NG*) and Lamivudine 5′-triphosphate (*LTP*). Formation of polyionic complex between anionic LTP and cationic NG is shown in the circle. **b** Transmission electron microimages of the CEPL core (*left image*) and NG/NTP nanodrug (*right image*) after vanadate staining. **c** NG/NTP demonstrated sustained drug release with linear in vitro kinetics (*right graph*; PBS, 25 °C)

cholesterol moieties in one CEPL molecule. EPL was derivatized using cholesterol chloroformate, and the water-soluble CEPL product was purified by dialysis. After sonication, CEPL immediately formed compact core particles of 10 nm in diameter. To attach PEG molecules of protective polymer shell around the core particles and brain-targeting peptide vectors, we used PEG reagents, $mPEG_{3500}$-NHS and maleimide-PEG_{3500}-NHS. These reagents react with amino groups of the CEPL core. Brain-specific peptides with N-terminal cysteine and C-terminal amide modifications could be covalently attached by reacting with maleimide moieties of the PEGylated nanogels (Fig. 2a). Hydrodynamic diameter (d_h) of NG in aqueous solution was less than 20 nm, however, peptide-modified nanogels showed a larger size of 32-35 nm (Table 1; and compare to TEM images in Fig. 2b).

An average peptide content in nanogels was 12±1 %, which corresponds to two peptides per nanogel in average, or derivatization rate of 70 %. Based on the size, larger peptide-modified particles could potentially represent a tetrahedral association of four smaller nanogels (e.g., see marked particles in Fig. 2b). Thus, vectorized nanodrugs may contain from 2 to 8 peptide molecules and be able to bind vascular targets on the BBB cooperatively and remain efficiently attached to the brain endothelium in hydrodynamic conditions of the blood flow.

NG/NTP Nanodrug Formulation

5′-Triphosphates of antiviral nucleoside analogs (NTP) act as active intermediates in the inhibition of HIV-1 reverse transcriptase (RT) through the DNA chain growth termination. We synthesized 5′-triphosphates of Zidovudine, Lamivudine and Abacavir (ZTP, LTP and BTP, respectively), components of therapeutic antiviral cocktails Combivir and Trizivir, using the previously developed method of chemical phosphorylation (Vinogradov et al. 2005a). Lamivudine was used with exocyclic amino group protected by isobutyryl group. All NTP have been purified by dialysis (MWCO 500) against water and precipitated as sodium salts in acetone solution of sodium perchlorate. Purity of NTP was usually higher than 70 %; other products were mostly di- and monophosphates, which are also active drugs, as determined by analytical ion-pair reverse phase HPLC (Galmarini et al. 2008). UV purity of these compounds was 90–95 % (NRTI content). Dry sodium salts of NTP samples could be stored in refrigerator with less than 5 % degradation in two years.

NG/NTP formulations have been prepared by mixing concentrated aqueous solutions of cationic NG and anionic NTP drugs (4:1 weight ratio). After isolation by gel filtration, NG/NTP complexes were obtained in lyophilized form. Drug content in the complexes was calculated from UV absorbance using extinction coefficients of NRTI (Table 1). All NG/NTP nanodrugs demonstrated good solubility in aqueous and serum-containing media and formed compact particles with narrow size distribution. In physiological conditions in vitro, NTP molecules could slowly dissociate from cationic network and diffuse out from the internal volume of nanogels. Complete NRTI release from nanodrugs showed practically linear kinetics and was over after 4 days of incubation (Fig. 2c).

Accumulation in Macrophages

Dominant cellular targets of antiviral nanodrugs are HIV-1 infected macrophages. Brain-associated macrophages and microglia were also found to contain integrated virus (Garden 2002). To evaluate drug accumulation efficacy in macrophages, we used an in vitro culture of human monocyte-derived macrophages (MDM). Cultured MDM were treated with Rhodamine-labeled nanogels loaded with cytidine 5′-triphosphate (CTP) as a model drug, and the cellular accumulation was analyzed by fluorescence-activated cell sorting (FACS). We observed an interesting phenomenon after the treatment with low concentration of nanodrugs (10 μg/mL). Nanodrug accumulation reached maximum after 1 h-treatment, but the amount of cell-associated nanodrug was then dropped significantly after 2 h-treatment (Fig. 3a). At higher nanodrug concentration (50 μg/mL), the accumulation curve also showed a downward bend after 30 min of incubation that was characteristic to cells with active drug efflux. Evidently, nanodrug accumulation in MDM is reversible; however, higher nanodrug levels can overcome this cellular efflux. It is still unclear whether this property can affect the antiviral efficacy of NG/NTP formulations at lower concentrations, for example, in the brain. We observed a significant 6-fold increase in MDM accumulation of nanodrug after 4 h-incubation at 50 μg/mL compared to its concentration in the medium.

MDM uptake of peptide-modified and non-modified NG/NTP was also compared. Glutathione was recently proposed as a potential vector for drug delivery to the central nervous system (CNS) (Geldenhuys et al. 2011). Glutathione-modified nanogels (50 μg/mL) demonstrated the initial fast uptake in MDM, which was directly proportional to the amount of glutathione moieties attached to the NG and mostly reached saturation after 4 h-treatment (Fig. 3b). Nanogel modification with peptide vectors could increase MDM accumulation 16-fold as compared to its concentration in the cellular medium.

Drug Release

Anionic NTP bind cationic nanogels via polyionic interactions, which are sensitive to ionic strength and the presence of counter-ions in the medium. Based on our in vitro drug release results, nanodrug administration could be performed every 3-4 days (Fig. 2c). We also investigated the intracellular drug release using laser confocal microscopy. The complex of

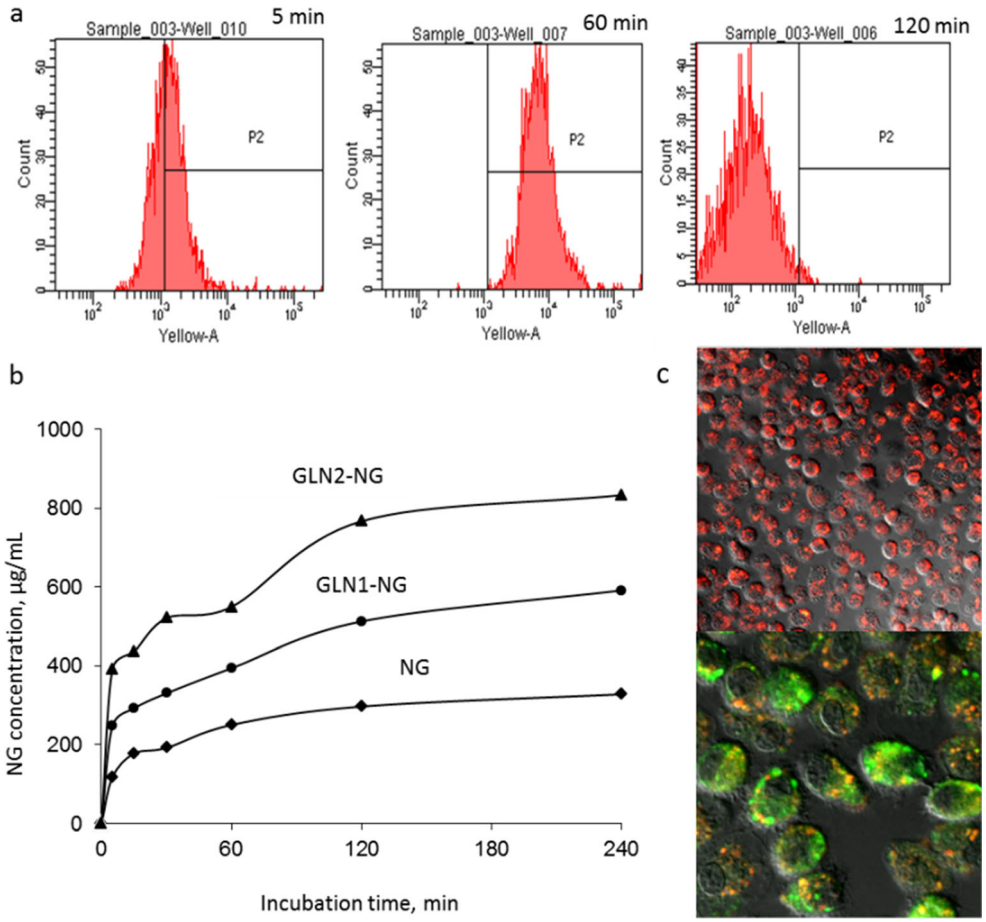

Fig. 3 Accumulation of Rhodamine-labeled nanogels (Rh-NG) in MDM. **a** FACS images obtained for the cells treated with Rh-NG concentration of 10 μg/mL. Initially internalized Rh-NG was ejected from MDM in 2 h. **b** Cellular uptake kinetics of Rh-NG and the carrier modified with glutathione vector (GLN1: 2.5 %, GLN2: 4.8 % peptide content) at concentration of 50 μg/mL. **c** Confocal microimages of cells treated for 1 h with empty Rh-NG (*top part*) or Rh-NG loaded with a 5′-triphosphate drug ATP-BODIPY FL (*green fluorescence*) at concentration 25 μg/mL (*bottom part*)

Rhodamine-labeled nanogel with Fluorescein-labeled ATP-BODIPY FL as a model drug was prepared, and its accumulation in MDM was monitored. Already in 30 min, we observed a significant increase in diffuse green fluorescence of free ATP drug in cytoplasm, while composite yellow fluorescence of ATP drug-loaded nanogels was mostly localized inside endosomes and on the cellular membrane. After 2 h-incubation, the amount of free drug was even more elevated in cytosol (Fig. 3c). The result shows that intracellular drug release occurs through an active membrane-related mechanism. Previously, we found that interaction of cationic nanogels with cellular membrane could induce a membrane fusion mechanism that resulted in fast NTP drug release directly into cytoplasm (Vinogradov et al. 2002). In case of cholesterol-modified cationic nanogels, this membrane interaction (fusion) can be even stronger due to the synergistic effect of both charge and lipophilic moiety, which accelerate intracellular drug release either directly through cellular membrane or from endosomes into cytoplasm (Guo et al. 2008).

Cytotoxicity in Brain-associated Cells

Cytotoxicity of NG/NTP formulations and multi-drug cocktails was evaluated in human neuroblastoma SH-SY5Y cells (neurons), human glioblastoma A172 cells (astrocytes), immortalized murine microglial BV-2 cells (microglia) and brain capillary endothelial bEnd3 cells (brain microvasculature). The standard MTT cytotoxicity assay was used to determine nanodrug concentrations when 50 % of treated cells survive (IC_{50} values). These cell lines have been pretreated for 4 h with serial dilutions of free and mixed NRTI, or NG/NTP obtained from non-modified or peptide-modified (ApoE and BP2) nanogels, and analyzed 24 h later. Survival curves plotted vs. drug/nanodrug concentrations were used to calculate IC_{50} values using a trapezoid rule (Table 2). Free drugs and combinations showed some toxicity (IC_{50} 100–800 μg/mL) only in microglial BV-2 cells, while in other cells IC50 values were higher than 1 mg/mL, representing a very low cytotoxicity. Unloaded ApoE-NG demonstrated medium toxicity in all cells (IC_{50} 200–500 μg/mL), while unloaded non-modified nanogel was practically non-toxic. NG/NTP showed no toxicity in all studied cells (IC_{50}> 1 mg/mL). Comparison of ApoE- and BP2-modified NG/NTP demonstrated that BP2-modified nanodrugs have equal to ApoE-modified nanodrugs toxicity in microglial cells, but are less toxic in neuronal cells and astrocytes (Table 2).

Table 2 Cytotoxicity of NRTI, NG/NTP and corresponding antiviral cocktails in brain-associated cells

Drug/nanodrug[a]	Neurons[b]	Astrocytes[b]	Microglia[b]	BBB[b]
Z	>1[c]	>1	0.8	>1
Z+L	>1	>1	0.2	>1
Z+L+B	>1	>1	0.1	>1
NG	>1	1	>1	>1
NG/ZTP	>1	>1	1	>1
NG/ZTP+LTP	1	>1	>1	–
NG/ZTP+LTP+BTP	>1	>1	>1	–
ApoE-NG	0.2	0.4	0.5	1
ApoE-NG/ZTP	0.1	0.01	1	0.8
ApoE-NG/ZTP+LTP	0.1	0.03	1	–
ApoE-NG/ZTP+LTP+BTP	0.06	0.09	0.9	–
BP2-NG/ZTP	1	>1	>1	>1
BP2-NG/ZTP+LTP	0.9	>1	>1	–
BP2-NG/ZTP+LTP+BTP	0.9	>1	>1	–

[a] IC_{50} values (mg/mL) determined by MTT assay after 24 h treatment

[b] Cellular models: SH-SY5Y (neurons), A172 (astrocytes), BV-2 (microglia), bEnd.3 (BBB)

[c] Formulations with IC_{50}>1 mg/mL are commonly considered as non-toxic

Neurotoxicity

To evaluate potential neurotoxicity of nanodrugs, we measured apoptosis in cultured SH-SY5Y neuronal cells treated with NG/NTP at antiviral EC_{90} concentrations using Annexin V-FITC/FACS method. In apoptotic cells, the FITC-labeled Annexin V protein specifically binds phosphatidylserine on the exposed inner membrane; fluorescent apoptotic cells are then counted by FACS. Unmodified NRTI, NG/NTP and NG/NTP vectorized with ApoE peptide induced low level of apoptosis 24 h after the treatment. Unloaded nanocarriers showed higher neurotoxicity, evidently, due to the high density of cationic groups present (Fig. 4a). Fortunately, proteolysis of the nanogels' EPL backbone in vivo should render them safe after the drug release. These results demonstrate that brain-targeted nanodrugs have good neurotoxicity profile and can be applied for the treatment of HIV-1 infection in the CNS.

Significant detrimental effect of high ROS levels on viability of neurons in the CNS was reported previously (Barzilai 2007). Potential neurotoxicity of nanodrugs associated with ROS formation was measured in primary rat neurons treated with NG/NTP at an effective antiviral concentration (Fig. 4b). While hydrogen peroxide, as a positive control, induced a 3-fold increase in ROS level in neurons, the NG alone wasn't active. Treatment with Abacavir (B) boosted two-fold the ROS level in the cells, which could potentially lead to neurotoxicity. Oppositely, treatment with NG/BTP and, especially, peptide-NG/BTP demonstrated a statistically significant lower accumulation of ROS in neurons.

Mitochondrial Toxicity

Depletion of mitochondrial DNA (mtDNA) is a measure of mitochondrial toxicity of many NRTI drugs causing neurotoxic side effects. HepG2 cells are a common model of new drug evaluation by mitochondrial toxicity. DNA content in treated cells was measured using a real-time SYBR Green PCR after a 10-days treatment with NG/ZTP and Z at concentration of 300 and 30 μg/mL, respectively. Nuclear DNA (nuDNA) was used as an internal standard. The ratio of mtDNA/nuDNA in isolated total DNA is normally constant, while in many NRTI-treated cells the ratio

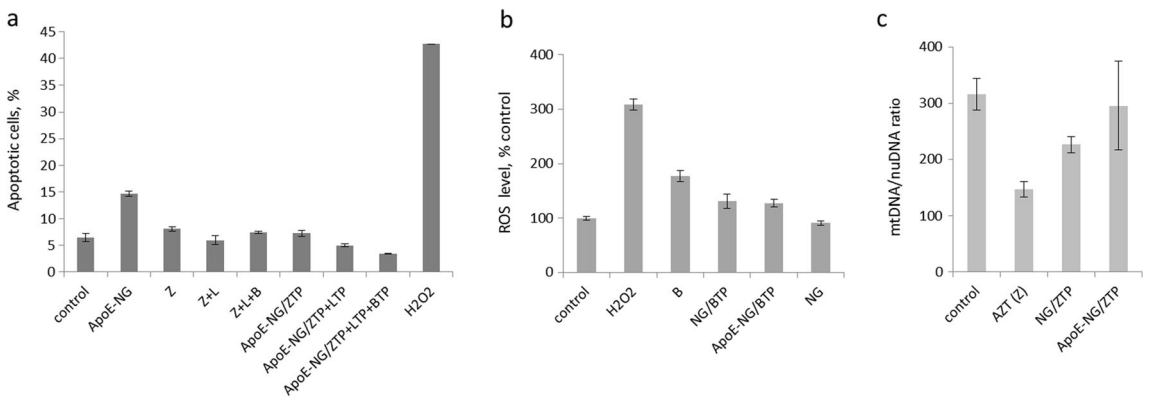

Fig. 4 Cytotoxicity of NG/NTP formulations. **a** Apoptosis in SH-SY5Y cells as a neuronal model after 24 h-treatment with Z, Z+L (2:1 wt) and Z+L+B (2:1:2 wt) cocktails with total concentration of 20 μg/mL; or ApoE-NG loaded with ZTP, ZTP+LTP (2:1 wt) and ZTP+LTP+BTP (2:1:2 wt) cocktails with total formulation concentration of 200 μg/mL (20 % NTP content). Data are means±SEM (n=3). **b** Formation of reactive oxygen species (ROS) after 24 h-treatment of rat neurons with formulations of NG/BTP and ApoE-NG/BTP (4 μg/mL), H_2O_2 (40 μM) and NG (4 μg/mL). Data are means±SEM (n=6). **c** Depletion of mitochondrial DNA (mtDNA) in hepatic HepG2 cells as a cellular model to measure mitochondrial toxicity of drugs after 10 days-treatment with AZT (30 μg/mL) and formulations of NG/ZTP and ApoE-NG/ZTP (300 μg/mL). Data are means±SEM (n=3)

becomes lower depended on drug toxicity. We observed a significant two-fold reduction in the mtDNA/nuDNA ratio for AZT and much lower 30 % reduction for NG/ZTP. Nearly no mitochondrial toxicity was observed for peptide-modified NG/ZTP (Fig. 4c). The used concentration corresponds to NG/NTP levels administered in vivo and required to obtain effective antiviral nanodrug concentrations in the brain, which are equivalent to the 10-fold reduction of antiviral activity (EC_{90}) achieved in HIV-infected MDM. Thus, brain-targeted peptide-NG/ZTP have evidently a significant neurological advantage over AZT in chronic treatment conditions.

Antiviral Activity

Antiviral efficiency of nanodrugs and multi-drug cocktails was compared as a dose-dependent RT activity in HIV-1 infected MDM at different time points post-infection. The cells were pretreated with NG/NTP for 4 h before inoculation with HIV-1_{ADA} strain. Viral RT activity in treated and non-treated HIV-1 infected MDM cells was analyzed by inclusion of ^{3}H-thymidine in DNA on Days 5 and 7. We evaluated antiviral efficacy of NG/NTP formulations: NG/ZTP, NG/LTP, NG/BTP, and their mixtures corresponding to Z : L ratio equal to 2 : 1 (similar to Combivir) and Z : L : B ratio equal to 2 : 1 : 2 (similar to Trizivir). Viral RT activity in treated infected MDM on Day 7 is shown as a percentage of the RT activity in non-treated infected cells (Fig. 5). Single drug NG/NTP formulations demonstrated strong antiviral activity (IC_{90}) at concentrations higher than 2 μg/mL, or 0.7 μM by NRTI, which was better or equivalent to the effective concentrations of free drugs (Fig. 5a, b). Modification of nanodrugs with a brain-specific peptide has not affected the efficacy of HIV-1 inhibition. Nanocarriers without drugs practically did not affect the RT activity.

The dual-drug NG/NTP formulations showed the same activity (IC_{90}) at lower concentrations 0.9-1.1 μg/mL, or 0.3 μM by NRTI. Triple-drug NG/NTP formulations were the most effective, with IC_{90} equal to 0.3-0.6 μg/mL, or 0.1–0.2 μM by NRTI (Fig. 5c, d). The equivalent activity of free NRTI could be achieved usually in the range of 0.4–1 μM. It is important to take into account that average NRTI content in nanoformulations was 10 %. Thus, NG/NTP were more effective than free drugs; nanoencapsulated Abacavir, for example, demonstrated equal to free drug HIV-1 inhibition efficacy at 4 to 7-fold lower drug level (Fig. 4d). Nanodrug combinations demonstrated a similar activity pattern compared to the

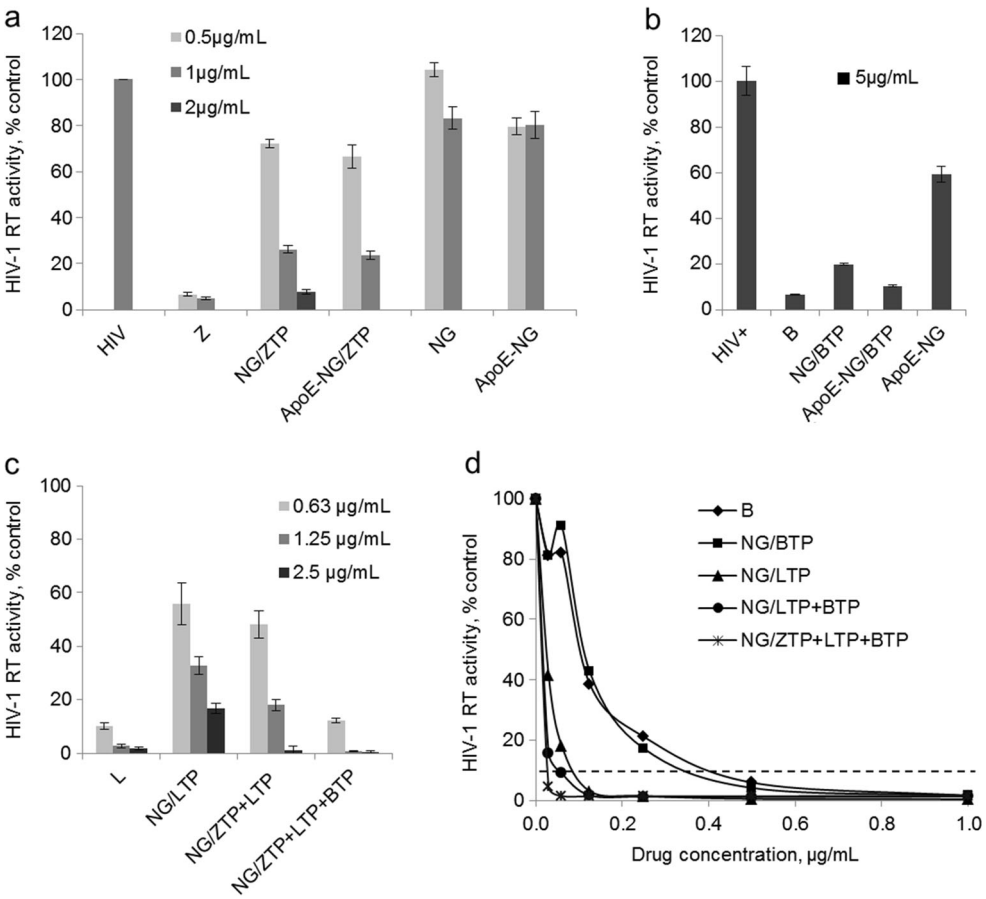

Fig. 5 Antiviral efficiency of NG/NTP formulations and nanodrug cocktails in HIV-1 infected MDM. **a–c** Inserts show the concentration of free NRTI (*Z*, *B*, *L*) or nanodrugs (*NG/ZTP*, *ApoE-NG/ZTP*, *ApoE-NG*, *NG/BTP*, *ApoE-NG/BTP*, *NG/LTP*, *NG/ZTP+LTP*, *NG/ZTP+LTP+BTP*). NRTI content in nanodrugs was ca.10 % (Table 1). **d** Comparison of single nanodrug (*NG/BTP*, *NG/LTP*), dual drug (*NG/LTP+BTP*) and triple drug (*NG/ZTP+LTP+BTP*) cocktails at different dilutions. The *dotted line* shows RT activity level correlating to EC_{90}. Data are means±SEM of two experiments

corresponding NRTI cocktails and suppressed HIV-1 RT activity to the minimal detection sensitivity of the assay.

Transport in Cellular BBB Model

We compared the effect of nanogel modification with brain-specific peptides on their ability to cross mature confluent monolayers of murine brain capillary endothelial cells (bEnd3) in the in vitro cellular BBB model (Brown et al. 2007). The bEnd3 cells (passages 32-34) were grown on Matrigel-treated porous inserts until confluency, when the electric conductivity of the cell monolayer significantly dropped and its resistance increased to a 45-50 Ohm/cm^2. Lucifer yellow internal standard was used to ensure the integrity of cell monolayers. Rhodamine-labeled non-vectorized nanogel and nanogels modified with glutathione, BP1 and BP2 peptides, ApoE and TGN peptides have been investigated in the BBB model in order to determine the most efficient peptide candidate for the efficient nanodrug delivery into the brain. Apparent permeability coefficient (P_{app}) values for empty and CTP-loaded vectorized nanogels are shown in Table 3. We found that cationic nanogels (without drug) have predominantly a higher permeability across the BBB than CTP-loaded neutral formulations. ApoE peptide increased permeability modified nanogels by 70 % compared to the non-modified nanogel. TGN peptide demonstrated very close efficacy. BP1 and BP2 peptide modifications resulted in two- and three-fold increases in permeability, respectively (Gerson et al. 2014). Surprisingly, short tripeptide GLN occupied the second place by the efficacy after BP2 peptide. The average peptide content in modified nanogels was 11 %, which equivalent to two peptide molecules per nanogel, but for GLN nanogels this number was two times higher. Potential formation of tetrahedral tetramers from vectorized nanogels, which have 8 peptide molecules in total, was concluded from light scattering data; this factor can significantly increase the affinity of receptor-mediated interaction of nanodrugs with the BBB endothelium.

Table 3 Apparent permeability coefficients of peptide-nanocarriers in bEnd.3 cellular model of the BBB

Nanogel[a]	P_{app}, cm/s (w/o CTP)	P_{app}, cm/s (with CTP)[b]
NG	$2.86\pm0.1\times10^{-6}$	$2.2\pm0.21\times10^{-6}$
GLN-NG	$6.29\pm0.65\times10^{-6}$	$5.04\pm0.6\times10^{-6}$
ApoE-NG	$4.55\pm0.49\times10^{-6}$	$3.75\pm0.11\times10^{-6}$
BP1-NG	$4.78\pm0.16\times10^{-6}$	$4.55\pm0.8\times10^{-6}$
BP2-NG	$7.58\pm0.59\times10^{-6}$	$6.56\pm0.26\times10^{-6}$
TGN-NG	$4.36\pm0.4\times10^{-6}$	$3.52\pm0.55\times10^{-6}$

[a] P_{app} coefficients of free NRTI: 1.67×10^{-6} (Z), 1.8×10^{-6} (L) and 0.54×10^{-6} (B)

[b] Nanogels loaded with a model triphosphate drug, CTP

Brain Accumulation In Vivo

We measured brain accumulation of BP2-peptide modified tritium-labeled nanogel (BP2-NG) after *i.v.* injection in C57/BL6 mice. Accumulation of radioactivity in the brain, blood and other organs was determined two hours and 6 h post-injection after animal sacrifice and perfusion. The data are shown in Fig. 6a. Brain accumulation was two times higher 6 h compared to 2 h post-injection (2 and 1.2 % ID/g, respectively), though the brain-to-blood ratio remained unchanged (2.4). After 2 h, the accumulation in various organs (lung, liver, spleen, kidney and heart) was ca. 4 % ID/g, but after 6 h it increased to 8–10 % ID/g on average. We evaluated the effect of NG modification by BP2 peptide on accumulation in the brain. BP2-NG demonstrated excellent 2.5 to 3-fold higher brain accumulation in comparison with non-modified NG. It can be seen in Fig. 6b that increasing the dose from 0.5 mg to 1 mg per mouse does not enhance significantly the brain accumulation of non-vectorized NG and BP2-NG 24 h post-injection. I.v. injection of free BP2 peptide 1 h prior the administration of BP2-NG evidently resulted in some increase of the number of binding sites on brain endothelium. Interestingly, at lower administered doses (0.5 mg/ mouse) we observed nearly two-times higher accumulation in the brain (%ID/g), while the brain/blood ratio was low (ca. 0.5). Higher nanodrug dose was associated with the higher brain/blood ratio (1.5-2). Effect of free BP2 peptide pre-injection on the blood/brain ratio was also well visible. We concluded that BP2-NG/NTP is a promising targeted nanodrug that is able to reach anti-HIV therapeutic levels in the CNS.

Discussion

Effective CNS delivery of many drugs, especially hydrophilic and negatively charged molecules, still remains an unsolved dilemma. Progress of nanotechnology and development of novel particulate drug delivery systems resulted in the extensive search for drug nanoformulations that competently cross the BBB. Despite many efforts, only a small fraction of administered nanocarriers could find its way into the brain. Cationic macromolecules and nanocarriers demonstrated efficient brain accumulation, however, high retention in lungs, liver and spleen, the organs with high presence of macrophages, and in the main filtering organ, kidney, was observed. PEGylated cationic nanocarriers, loaded with negatively charged drugs, demonstrated longer blood circulation and better chances to penetrate the BBB (Kabanov and Batrakova 2004). Cationic nanogels built from PEGylated cationic polyethylenimine (PEI) networks have emerged as a

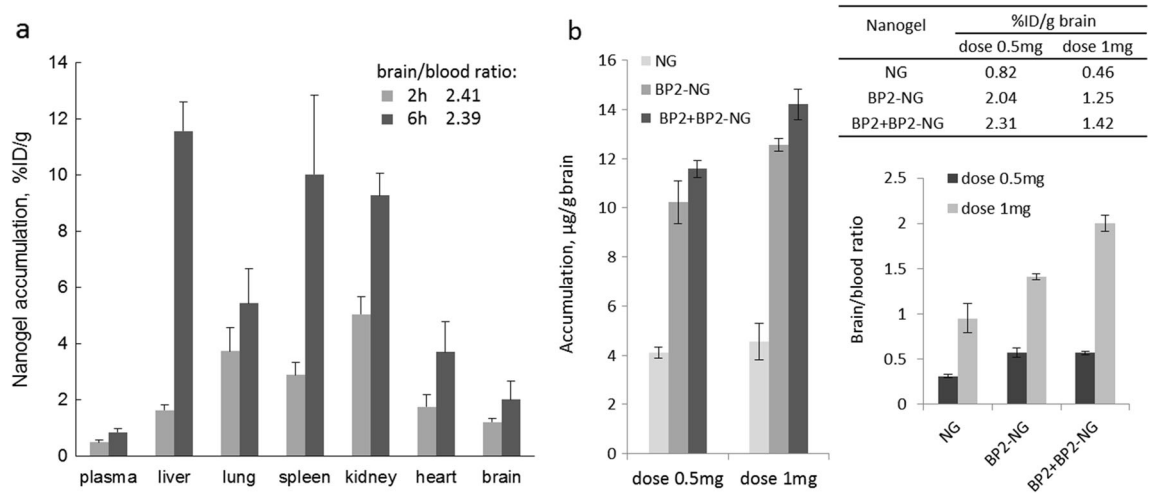

Nanogel	%ID/g brain	
	dose 0.5mg	dose 1mg
NG	0.82	0.46
BP2-NG	2.04	1.25
BP2+BP2-NG	2.31	1.42

Fig. 6 Biodistribution and brain accumulation of BP2 peptide-modified nanogels. ^{3}H-labeled nanogels have been injected in tail vein of C57/BL6 mice. **a** Organs were harvested at 2 and 6 h, or **b** 24 h post-injection. Data are means±SEM (four animals per group). Nanogels (*NG*, *BP2-NG*) were injected at doses: **a** 1 mg, or **b** 0.5 and 1 mg per mouse (equal to 20 and 40 mg/kg). Nanogels levels in organs are shown as a percentage of injected dose per gram (%ID/g), or in µg/g brain. The brain/blood ratio was calculated using nanogel levels in the brain and serum at the specific time points. BP2+ means *i.v.* injection of 1 mg of free BP2 peptide 1 h before the injection of ^{3}H-labeled BP2-NG in mice

promising drug delivery system to the CNS (Vinogradov et al. 2004a), as well as for encapsulation of 5′-triphosphates of nucleoside analogs (Vinogradov et al. 2005b). Among other nanodelivery approaches, entrapment of ZTP with PEI and encapsulation of the complex in poly(iso-butylcyanoacrylate) nanocapsules is worth to mention. These nanocapsules efficiently delivered ZTP to macrophages in vitro, reaching relevant cellular concentrations for therapeutic purposes (Hillaireau et al. 2006).

Recent investigations of the fate of different nanoparticles in vivo showed strong dependence of the CNS accumulations on the particle size (Sonavane et al. 2008). Smaller metal nanoparticles penetrated the BBB much more efficiently and exhibited higher neurotoxicity. Smaller nanoparticles were also found to migrate farther from capillaries in the brain tissue (Zhou et al. 2013). The size (d_h) range for best CNS penetrating nanocarriers was 20–70 nm. We observed that the size affected the retention of loaded cationic nanogels in organs: the maximum retention was observed for particles with the diameter between ca.100 and 200 nm. Thus, to reach the efficient penetration of nanodrugs into the brain, small and uniform particles with d_h 20–40 nm have to be manufactured. Many micellar systems, e.g., polymer-lipid amphiphilic conjugates produce small nanoparticles in this size range (Torchilin 2001). Another example, Pluronic-PEI conjugates could be readily converted to micellar nanogels after sonication and cross-linking in aqueous system (Vinogradov et al. 2004b). In this paper, we applied the micellar architecture to produce very small cationic nanogels starting from a new biodegradable and biocompatible material, epsilon-polylysine (EPL). Biosynthetic EPL is a linear cationic polymer (Mw 4600) with antimicrobial activity that found applications mostly as a non-toxic food additive (Hamano 2011). Compared to normal L-polylysine, it is significantly less toxic and can be produced microbiologically in large amount and with narrow polydispersity. Previously, an application of amphiphilic octenyl-EPL in the form of micellar nanocarriers for delivery of poorly soluble curcuminoids was reported (Yu et al. 2011). We found that cholesterol-modified EPL in aqueous solution can form compact cationic particles after sonication due to the formation of internal cholesterol clusters. Non-vectorized or vectorized nanogels are easily produced from these particles by modification with multifunctional PEG linkers. Small nanodrugs (d_h 20–30 nm) can be produced after loading these nanogels with anionic drugs, e.g., 5′-triphosphates of antiviral NRTI.

NRTIs are major components of anti-HIV multidrug cocktails and efficiently reduce viral titer in the blood. However, many of them, e.g., Zidovudine and Abacavir, have very low BBB penetration due to drug efflux transporters expressed on the BBB endothelium (Shaik et al. 2007; Eilers et al. 2008). Therefore, the NRTI levels in the CNS are usually inadequate to significantly reduce the HIV-1 activity. Increase in dosage can alleviate this obstacle, but is accompanied by serious side effects, such as peripheral neurotoxicity resulted from NRTI-related mitochondrial toxicity (Feeney and Mallon 2010). Failure to treat HIV-1 infection in the brain leads to more frequent occurrences of neuropathological disorders during the life-long antiviral therapy (Lindl et al. 2010). Novel therapeutic drugs able to boost the antiviral therapy in the CNS and reduce toxicity associated with increased NRTI dosages are in great demand. We recently suggested therapeutic application of NRTI 5′-triphosphates, which could have limited accumulation in mitochondria due to their negative charge.

Various NG/NTP were tested in HIV-1 infected macrophages and demonstrated several times more efficient inhibition of the virus than free NRTI (Vinogradov et al. 2010). Vectorized nanogels could deliver these drugs into the brain and induce 10-fold suppression of HIV-1 activity in the CNS following the systemic two weeks treatment (Gerson et al. 2014). However, the NG/NTP must be produced from biodegradable and more biocompatible materials than PEI to be applied for the therapy of human patients. Novel CEPL-based nanogels meet the requirements, and all studied nanodrug cocktails demonstrated high antiviral efficacy, as well as low mitochondrial and neuronal toxicities.

Consistent progress is being made in application of novel brain-specific vectors attached via a linker to drug delivery systems, which can enter the CNS via receptors on the luminal surface of brain capillary endothelial cells. Although these receptors may not be expressed only on the BBB, this approach can significantly enhance otherwise poor drug accumulation in the brain. Different proteins and receptor-specific antibodies, as well as certain small molecules using brain transporters, have been studied with various degree of success (Georgieva et al. 2014). One of the requirements for the efficient CNS drug delivery is high density of these receptors, which could support an adequate mass transport into the brain. However, immunological limitations associated with non-humanized proteins make their application complicated. Short peptides usually do not induce immune response; therefore, recently effective selection approaches for peptide binding endothelial receptors have been developed (Powell Gray and Brown 2014). Brain-targeting of nanodrugs using convenient peptide vectors would create excellent nanodrug candidates for the advanced treatment of HIV infection in the CNS. Several promising vectors, targeting specific receptors expressed on the BBB endothelium, were recently identified by using phage display approach. Apolipoprotein E receptor is specific for the BBB and was shown to allow delivery of ApoE-modified nanocarriers into the brain (Zensi et al. 2009). Recently, we successfully used a short peptide binding the ApoE receptor (Sauer et al. 2005) to vectorize cationic nanocarriers for CNS delivery (Zhang et al. 2010; Vinogradov et al. 2010). Here, we compared several reported combinatorially selected peptides as vectors for nanogel delivery into the brain. Two brain-binding peptides (BP1 and BP2) have been identified using in vivo panning from 7-mer peptide phage display library (Sadanandam et al. 2007). We found that BP2 peptide was the most efficient one when used in modification with NG/NTP in comparison to other tested peptides in delivery of nanodrugs across the in vitro bEnd.3 model of the BBB (Table 3). In addition, BP2-modified NG/NTP showed a much lower neurotoxicity than ApoE-modified NG/NTP and, thus, can be considered as potential candidates for translational preclinical research.

Important information was obtained in this research about antiviral activity of multi-nanodrug cocktails, modelling therapeutic dual- or triple-drug NRTI cocktails, such as Combivir and Trizivir. When RT inhibition by individual NG/NTP and NG/NTP combinations was compared to free NRTI and drugs cocktails in cultured HIV-1 infected MDM, the nanodrug combinations were found to have similar or higher efficacy based on the effective drug concentration resulting in 10-fold reduction of RT activity (EC_{90}). On average, 5-fold higher therapeutic levels of nanodrugs compared to EC_{90} levels observed in the infected MDM could be reached in the brain even 24 h after the systemic administration of BP2-NG/NTP. The reported here nano-NRTI approach is the further step to adequate treatment of HIV-1 infection in the brain. These novel nanodrugs will be next studied in vivo in order to determine optimal parameters of systemic administration, reduced peripheral toxicity, high brain accumulation, and efficient therapeutic activity against HIV-1 infection and HIV-related inflammation in the CNS.

Acknowledgments Authors acknowledge financial support from National Institute of Neurodegenerative Diseases and Stroke (grant NS076386 to S.V.V. and S.G.). The content is solely the responsibility of the authors and does not necessarily represent the official views of the National Institutes of Health.

Ethical Standards Animal studies were performed according to the principles of animal care outlined by the National Institutes of Health, and protocols were approved by the Institutional Animal Care and Use Committee at University of Nebraska Medical Center. Female C57BL/6 mice (age 8 weeks) used in experiments were purchased from Charles River Laboratories (Wilmington, MA) and maintained under sterile conditions in controlled setting.

Conflict of Interest The authors declare that they have no conflict of interest.

References

Bagasra O, Lavi E, Bobroski L, Khalili K, Pestaner JP, Tawadros R, Pomerantz RJ (1996) Cellular reservoirs of HIV-1 in the central nervous system of infected individuals: identification by the combination of in situ polymerase chain reaction and immunohistochemistry. AIDS 10:573–585

Barzilai A (2007) The contribution of the DNA damage response to neuronal viability. Antioxid Redox Signal 9:211–218

Brown RC, Morris AP, O'Neil RG (2007) Tight junction protein expression and barrier properties of immortalized mouse brain microvessel endothelial cells. Brain Res 1130:17–30

Delehanty JB, Boeneman K, Bradburne CE, Robertson K, Bongard JE, Medintz IL (2010) Peptides for specific intracellular delivery and targeting of nanoparticles:implications for developing nanoparticle-mediated drug delivery. Ther Deliv 1:411–433

Eilers M, Roy U, Mondal D (2008) MRP (ABCC) transporters-mediated efflux of anti-HIV drugs, saquinavir and zidovudine, from human endothelial cells. Exp Biol Med (Maywood) 233:1149–1160

Feeney ER, Mallon PW (2010) Impact of mitochondrial toxicity of HIV-1 antiretroviral drugs on lipodystrophy and metabolic dysregulation. Curr Pharm Des 16:3339–3351

Galmarini CM, Warren G, Kohli E, Zeman A, Mitin A, Vinogradov SV (2008) Polymeric nanogels containing the triphosphate form of cytotoxic nucleoside analogues show antitumor activity against breast and colorectal cancer cell lines. Mol Cancer Ther 7:3373–3380

Garden GA (2002) Microglia in human immunodeficiency virus-associated neurodegeneration. Glia 40:240–251

Geldenhuys W, Mbimba T, Bui T, Harrison K, Sutariya V (2011) Brain-targeted delivery of paclitaxel using glutathione-coated nanoparticles for brain cancers. J Drug Target 19:837–845

Georgieva JV, Hoekstra D, Zuhorn IS (2014) Smuggling drugs into the brain: an overview of ligands targeting transcytosis for drug delivery across the blood–brain barrier. Pharmaceutics 6:557–583

Gerson T, Makarov E, Senanayake TH, Gorantla S, Poluektova LY, Vinogradov SV (2014) Nano-NRTIs demonstrate low neurotoxicity and high antiviral activity against HIV infection in the brain. Nanomedicine 10:177–185

Guo XD, Tandiono F, Wiradharma N, Khor D, Tan CG, Khan M, Qian Y, Yang YY (2008) Cationic micelles self-assembled from cholesterol-conjugated oligopeptides as an efficient gene delivery vector. Biomaterials 29:4838–4846

Hamano Y (2011) Occurrence, biosynthesis, biodegradation, and industrial and medical applications of a naturally occurring ε-poly-L-lysine. Biosci Biotechnol Biochem 75:1226–1233

Henn A, Lund S, Hedtjärn M, Schrattenholz A, Pörzgen P, Leist M (2009) The suitability of BV2 cells as alternative model system for primary microglia cultures or for animal experiments examining brain inflammation. ALTEX 26:83–94

Hillaireau H, Le Doan T, Appel M, Couvreur P (2006) Hybrid polymer nanocapsules enhance in vitro delivery of azidothymidine-triphosphate to macrophages. J Control Release 116:346–352

Höschele D, Wiertz M, Garcia Moreno I (2008) A duplex real-time PCR assay for detection of drug-induced mitochondrial DNA depletion in HepG2 cells. Anal Biochem 379:208–210

Hunter AC, Moghimi SM (2010) Cationic carriers of genetic material and cell death: a mitochondrial tale. Biochim Biophys Acta 1797:1203–1209

Kabanov AV, Batrakova EV (2004) New technologies for drug delivery across the blood brain barrier. Curr Pharm Des 10:1355–1363

Kohli E, Han H-Y, Zeman AD, Vinogradov SV (2007) Formulations of biodegradable Nanogel carriers with 5′-triphosphates of nucleoside analogs that display a reduced cytotoxicity and enhanced drug activity. J Control Release 121:19–27

Lewis W, Day BJ, Copeland WC (2003) Mitochondrial toxicity of NRTI antiviral drugs: an integrated cellular perspective. Nat Rev Drug Discov 2:812–822

Li J, Feng L, Fan L, Zha Y, Guo L, Zhang Q, Chen J, Pang Z, Wang Y, Jiang X, Yang VC, Wen L (2011) Targeting the brain with PEG-PLGA nanoparticles modified with phage-displayed peptides. Biomaterials 32:4943–4950

Lindl KA, Marks DR, Kolson DL, Jordan-Sciutto KL (2010) HIV-associated neurocognitive disorder: pathogenesis and therapeutic opportunities. J Neuroimmune Pharm 5:294–309

Nukuna A, Gendelman HE, Limoges J, Rasmussen J, Poluektova L, Ghorpade A, Persidsky Y (2004) Levels of human immunodeficiency virus type 1 (HIV-1) replication in macrophages determines the severity of murine HIV-1 encephalitis. J Neurovirol 10(Suppl 1):82–90

Pialoux G, Fournier S, Moulignier A, Poveda JD, Clavel F, Dupont B (1997) Central nervous system as a sanctuary for HIV-1 infection despite treatment with zidovudine, lamivudine and indinavir. AIDS 11:1302–1303

Powell Gray B, Brown KC (2014) Combinatorial peptide libraries: mining for cell-binding peptides. Chem Rev 114:1020–1081

Sadanandam A, Varney ML, Kinarsky L, Ali H, Mosley RL, Singh RK (2007) Identification of functional cell adhesion molecules with a potential role in metastasis by a combination of in vivo phage display and in silico analysis. OMICS 11:41–57

Sauer I, Dunay IR, Weisgraber K, Bienert M, Dathe M (2005) An apolipoprotein E-derived peptide mediates uptake of sterically stabilized liposomes into brain capillary endothelial cells. Biochemistry 44: 2021–2029

Senanayake TH, Warren G, Wei X, Vinogradov SV (2013) Application of activated nucleoside analogs for the treatment of drug-resistant tumors by oral delivery of nanogel-drug conjugates. J Control Release 167:200–209

Shaik N, Giri N, Pan G, Elmquist WF (2007) P-glycoprotein-mediated active efflux of the anti-HIV1 nucleoside abacavir limits cellular accumulation and brain distribution. Drug Metab Dispos 35:2076–2085

Simon MJ, Cancel LM, Shi ZD, Ji X, Tarbell JM, Morrison B 3rd, Fu BM (2010) Permeability of endothelial and astrocyte cocultures: in vitro blood-brain barrier models for drug delivery studies. Ann Biomed Eng 38:2499–2511

Sonavane G, Tomoda K, Makino K (2008) Biodistribution of colloidal gold nanoparticles after intravenous administration: effect of particle size. Colloids Surf B: Biointerfaces 66:274–280

Tiwari SB, Amiji MM (2006) A review of nanocarrier-based CNS delivery systems. Curr Drug Deliv 3:219–232

Torchilin VP (2001) Structure and design of polymeric surfactant-based drug delivery systems. J Control Release 73:137–172

Vinogradov SV, Bronich TK, Kabanov AV (2002) Nanosized cationic hydrogels for drug delivery: preparation, properties and interactions with cells. Adv Drug Deliv Rev 54:135–147

Vinogradov SV, Batrakova EV, Kabanov AV (2004a) Nanogels for oligonucleotide delivery to the brain. Bioconjug Chem 15:50–60

Vinogradov SV, Batrakova EV, Li S, Kabanov AV (2004b) Mixed polymer micelles of amphiphilic and cationic copolymers for delivery of antisense oligonucleotides. J Drug Target 12:517–526

Vinogradov SV, Kohli E, Zeman AD (2005a) Cross-linked polymeric nanogel formulations of 5′-triphosphates of nucleoside analogues: role of the cellular membrane in drug release. Mol Pharm 2:449–461

Vinogradov SV, Zeman AD, Batrakova EV, Kabanov AV (2005b) Polyplex Nanogel formulations for drug delivery of cytotoxic nucleoside analogs. J Control Release 107:143–157

Vinogradov SV, Poluektova LY, Makarov E, Gerson T, Senanayake MT (2010) Nano-NRTIs: efficient inhibitors of HIV type-1 in macrophages with a reduced mitochondrial toxicity. Antivir Chem Chemother 21:1–14

Yu H, Li J, Shi K, Huang Q (2011) Structure of modified ε-polylysine micelles and their application in improving cellular antioxidant activity of curcuminoids. Food Funct 2:373–380

Zensi A, Begley D, Pontikis C, Legros C, Mihoreanu L, Wagner S, Büchel C, von Briesen H, Kreuter J (2009) Albumin nanoparticles targeted with Apo E enter the CNS by transcytosis and are delivered to neurones. J Control Release 137:78–86

Zhang H, Gerson T, Varney ML, Singh RK, Vinogradov SV (2010) Multifunctional peptide-PEG intercalating conjugates: programmatic of gene delivery to the blood-brain barrier. Pharm Res 27:2528–2543

Zhou J, Patel TR, Sirianni RW, Strohbehn G, Zheng MQ, Duong N, Schafbauer T, Huttner AJ, Huang Y, Carson RE, Zhang Y, Sullivan DJ Jr, Piepmeier JM, Saltzman WM (2013) Highly penetrative, drug-loaded nanocarriers improve treatment of glioblastoma. Proc Natl Acad Sci U S A 110:11751–11756